

Journal of Thermal Engineering

Web page info: https://jten.yildiz.edu.tr DOI: 10.14744/thermal.0001041



Research Article

Prediction of dual-axis solar tracking of the PV system for optimal power output using GA, DE, TLBO, Jaya, and Rao-3 algorithms

Mukesh KUMAR¹, PRABHANSU^{1,*}

¹Department of Mechanical Engineering, Sardar Vallabhbhai National Institute of Technology Surat, 395007, India

ARTICLE INFO

Article history Received: 23 September 2024 Accepted: 27 December 2024

Keywords:

Dual-axis Solar Tracker; Electrical Power; Simulation; Tilt Angle; Azimuth Angle

ABSTRACT

In this study, novel algorithms approach that forecast the sun's movement more accurately, even in bad weather, and optimize for additional characteristics besides solar tracking. It was investigated through comparative analysis by using standard optimization methods, i.e., the JAYA algorithm, Teaching Learning Based Optimization algorithm, Rao-3 algorithm, Genetic algorithm, and Differential Evolution algorithm for a dual-axis solar tracking of a Photovoltaic system. This dual-axis tracking involves rotation of two-axis, i.e., tilt angles and azimuth angles, to maximize the total available solar radiation at optimized tilt angles and azimuth angles for varying time from sunrise to sunset. The reason for obtaining optimum angles is to align the solar PV panel with the incoming solar radiation to get the maximum output. A non-linear and constrained optimization problem is employed to evaluate the optimum tilt angle and optimum azimuth angle trajectories. As in this case, the objective function is in an explicit form that is not known, the optimization methods are employed to evaluate the objective function, and that method calculates the available total solar radiation tracked and carried out in MATLAB software. The optimization results for the considered algorithms showed that the output electrical energy with the dual-axis tracker is far greater than that of the fixed system. It was found that for summer days, the electrical power generation by different optimization algorithms are as follows: TLBO-16.1713 kWh, JAYA-16.1436 kWh, Rao-3-16.1125 kWh, DE-16.2079 kWh, and GA-16.1969 kWh, and measured fixed system-13.2610 kWh. The obtained results for various optimization algorithms, in comparison to a measured fixed system, demonstrated significant enhancements in power generation.

Cite this article as: Kumar M, Prabhansu. Prediction of dual-axis solar tracking of the PV system for optimal power output using GA, DE, TLBO, Jaya, and Rao-3 algorithms. J Ther Eng 2025;11(6):1741–1755.

Statement of novelty and industrial relevance

Novel algorithms approach that forecast the sun's movement more accurately, even in bad weather, and optimize for additional characteristics besides solar tracking. Dual-axis

trackers that optimize efficiency and cost by combining fixed and single-axis features.

Enhanced Energy Generation: Dual-axis trackers boost solar system energy capture by 30-45% over fixed tilt

This paper was recommended for publication in revised form by Editor-in-Chief Ahmet Selim Dalkilic



^{*}Corresponding author.

^{*}E-mail address: prabhansu@med.svnit.ac.in

systems and 10-20% over single-axis trackers. They maximise solar capture by keeping the panels perpendicular to the sun all day and year.

Land Efficiency: Higher panel energy output allows for more electricity generation on less land. This helps in locations with high land costs or limited space.

Adaptability: They can be employed in regions where the sun's yearly path presents significant challenges in terms of capturing maximum energy.

Optimal results in Diverse Latitudes: Dual-axis trackers perform best in higher or lower latitudes when the sun angle fluctuates dramatically throughout the year.

Economic Value: Despite the greater upfront expenditures, the enhanced energy yield might result in faster returns on investment. The initial outlay may be higher, but the additional energy production should eventually pay for itself through economies of scale and technical developments.

INTRODUCTION

Renewable energy sources are gradually replacing fossil fuels and are the need of the hour. These are mainly derived from natural resources, either abundant in nature or constantly replenished. Renewable energy resources come from natural resources like wind, sun, waves, tides, and geothermal heat and are clean and pollution-free. Among the various renewable energy resources, solar energy is the most pristine and abundant in countries like India.

A PV cell is an electronic gadget that directly converts the sun's radiation into electrical power. A PV system's performance depends on the solar cells' temperature, which determines how efficiently they operate [1]. There are three selected parameters that determine the solar cell outputs. The photovoltaics selected parameters such as short circuit current (Isc), open circuit voltage (Voc), and maximum power (Pmax) are presented in [2,3]. The PV panel's efficiency decreases with the increased operating temperature of the module. According to Koundinya et al. (2017), the finned heat pipe can overcome the operating temperature of PV modules. It was also found that the experimental and computation study results are in good agreement [4]. Significant disadvantages of solar PV systems include high costs compared to fossil fuels, poor efficiency, and intermittent operation. In order to overcome these challenges, capturing more and more energy from the sun with the existing PV modules is a challenging task for researchers and the scientific community across the globe. PV materials, geographical locations, environment temperature, weather conditions, angle of incidence, and module direction influence the PV system's energy output. Tracking techniques decide the best orientation of the PV modules towards the sun. The intelligent tracking technique is the most promising among the several existing categories of tracking systems. It is because of its capacity to forecast the correct path of the sun by using predefined algorithms, as mentioned in

[5,6]. The variation in the solar intensity on the PV system exists because of daily and seasonal movements of the earth across the sun. The best possible orientation of solar panels to the trajectories of the sun can be achieved by considering the rotation as well as the revolution of the earth. With the optional use of solar trackers, collected solar energy can be increased by 10 to 100%, depending upon geographical locations and changing weather conditions. The only issue is that this tracking device consumes power equivalent to 2-3% of the increased power output [7]. An experimental study on the solar tracker using a sun tracking system to maximize the productivity of solar still was conducted by Abdallah et al. (2008). The solar tracking system under consideration was computerized and was used to orient the solar system, still having an effect of 1m² with the trajectory of the sun's movement throughout the day. The performance of the solar still with the single-axis tracker increased productivity by around 22%, which was greater than the static system under consideration [8]. An experimental study of dual axis solar tracker using a predefined Differential Evolution algorithm for tracking the sun's path throughout the day was done by Seme and Štumberger (2011). It was found that the maximum solar energy of the photovoltaic system was obtained by maintaining the optimum tilt and azimuth angles evaluated by the optimization technique. The results reported in this research showed that by using novel technologies, the efficiency of energy generation inside a PV system could be increased up to 10-50% [9,10]. In another investigation in a fixed system, the energy generation predicted through GA increased by 15.85% for PV modules [11]. The new method for optimizing solar trackers by applying arbitrary design and geometry of Concentrating Photovoltaic (CPV) and PV tracker system that moves less and requires less mechanical effort is now being used to track the sun's location. The optical system used in the solar tracking concentrator quickly reacts to variations in the sun's location throughout the day, month, and year. The goal of a solar tracking system is to hold onto solar light alignment with the surface of the receiver [12-14]. A fixed system and a continuous dual-axis sun tracking system based on a solar map and light-dependent resistor (LDR) sensors were evaluated in terms of power gain and system power consumption. It was discovered that compared to a continuous two-axis sun tracking system, the energy gain from a hybrid sun tracker is essentially non-existent. The proposed design system was found to have low energy consumption, high precision, and low cost [15]. The closed loop tracker was investigated with LDR sensors as input to the solar system. In contrast, in the case of an open loop system, a controller provides the driving signal to the servo motor based on current data inputs and the operating algorithm of the system. On days with cloudy conditions and days with clear skies, the proposed system may produce 12.8% and 26.9% more electricity than a static PV system. A dual axis with an open-loop solar tracker was also found to be automated and deployable anywhere on the plane

[16,17]. There are various tracking methods, but passive and active systems are the most common. In Passive systems, low-boiling-point gaseous liquids drive the system using the received solar radiation. On the other hand, active systems use gears and motors to manage PV modules. They are further classified into five driving systems: intelligent driving, Sensor driving, open-closed loop driving, microprocessor driving, and other combination driving based on the driving mechanisms used. Intelligent driver systems are one of the most used tracking systems nowadays because they use learning algorithms to forecast the precise location of the sun [18]. In another work, the optimum tilt and azimuth angles for the dual-axis tracker were used to optimize the power received by applying Harmony Search (HS) meta-heuristic algorithm. Based on the Julian date model, the performance was checked on six Chinese cities with diverse temperature zones to find the monthly optimum tilt and azimuth angles. The result was very close to the standard values [19]. A comparative study of the performance of the fixed, single-axis, and dual-axis solar tracking system over the year concluded that the generated electricity was found to be 2.25 MWh, 3.04 MWh, and 3.17 MWh, respectively. The single-axis tracking system produced about 35.30% more energy than the static system, while dual-axis solar tracker produced about 41.07% more than the static system under the same conditions. Fahad et al. (2019) concluded that the dual-axis tracker generated 3.96% more power than the single-axis tracker without considering the cloud. When the cloud effect was considered, the difference was reduced to 3.44% [20]. Due to the increasing demand for sustainable and green energy resources, Zaher et al. (2018) proposed an intelligent approach to optimize the orientation of continuous solar tracking systems on cloudy days. It was based on a 5-megapixel ground-based sky camera named 5481 VSE-C and provided by IDS imaging. It was equipped with a Fujinon fisheye lens and protected by a waterproof enclosure manufactured by automation and a fuzzy inference system. The experimental result for Perpignan city has efficiency gains of up to 9% relative to conventional continuous sun tracking systems under overcast conditions [21]. Saymbetov et al. (2021) developed a dual-axis schedule solar tracker with an adaptive algorithm to capture direct sunlight and maximize electrical power. It consists of a polycrystalline solar panel with a power of 60 W, an electric linear actuator, DC motor SV35-130/HP5 BFN, Atmega 328 microcontroller where a tracking algorithm was installed. The experimental work revealed that the amount of electrical power produced by the dual-axis schedule tracker with an adaptive algorithm in October and November was 58.55 WH and 82.54 WH, respectively [22]. In order to design a low-cost hybrid system to deliver the required thermal energy for heating water and street lighting, a parabolic collector combined with a dual-axis tracking mechanism with an LDR sensor was used to move the parabolic dish with the movement of the sun. The experimental work revealed that the thermal efficiency using dual-axis and single-axis tracking mechanisms was 32.2% and 23.6%, respectively, with the same operating parameters [23]. This study focuses on the design and development of a dual-axis solar tracker using SIMULINK and SolidWorks. The tracker employs an LDR-based algorithm to monitor the sun's trajectory in real-time, utilizing time and location data. Results show that the tracking PV system produces more current than a static system, and the stand designed for 335-watt panels is strong enough to endure various wind conditions [24]. Another system, managed by a microcontroller, tracks the sun's position on both axes, with IoT monitoring for performance and alerts [25]. Additionally, a novel solar tracking system using a particle filter (PF) algorithm improves energy generation by 20.1% compared to fixed systems after a 60-day trial [26]. A dualaxis tracker with ESP8266 and LDR sensors enhances energy absorption and provides real-time monitoring of system data like temperature and power, with potential upgrades such as AI and remote monitoring [27]. D.A. Flores-Hernández D et al. 2024, this study presents a realtime tracking algorithm for dual-axis solar trackers, resulting in a 53.33% reduction in tracking movements, 60.77% reduction in operation time, and 14.18% decrease in energy consumption, while maintaining energy productivity. The tracker's energy consumption remains between 2% and 3% of the energy gain, ensuring profitability. Experimental findings show a mean tracking error of 4.61° (DMA) compared to 2.04° (CA), with azimuthal errors of 1.43° (DMA) and 0.27° (CA), and elevation errors of 4.39° (DMA) and 1.00° (CA). This method extends the tracker's lifetime by 6.8 times and integrates predictive maintenance through real-time data for improved durability and efficiency [28]. N. Koshkarbay et al. 2024 developed an adaptive control system for dual-axis solar trackers to optimize performance under varying weather conditions, using Clear Sky Index (CSI) thresholds and machine learning models for power output prediction with 99.3% accuracy. This system, integrating CSI-based decisions and forecasting, demonstrated energy generation improvements of 18.3% over horizontal configurations, 14.9% over single-axis trackers, and 10.01% over dual-axis trackers [29]. P. N. Praveen et al. 2024, proposed a dual-axis solar tracking system that combines an artificial neural network with an advanced particle swarm optimization method to improve energy forecasting accuracy. It uses meteorological data from Alice Springs and features innovative hidden layers for day/night data selection and input relevance. This approach enhances both ANN training and prediction performance. Future work will focus on multi-output fuzzified systems and further optimization improvements [30]. S.E. Bousbia Salah et al. 2024, introduced a solar dryer featuring a dual-axis tracking system and a parabolic trough concentrator, demonstrating efficient drying of apricots under desert conditions. The system achieved temperatures of up to 115°C, with an average thermal efficiency of 25.93%, and reduced the moisture content of apricots by 71.76%. Economic analysis

showed a low capital cost and a payback period of 0.43 years, highlighting its potential for widespread use in agricultural drying [31]. K. Kumba et al. 2024, explored the effectiveness of various solar tracking systems in enhancing energy output from photovoltaic panels, emphasizing dual-axis and hybrid trackers. It highlights advancements in tracking technologies, including machine learning and IoT integration, to improve energy capture efficiency. The research identifies key challenges and suggests future improvements, such as hybrid systems, cost-reduction strategies, and policy support, which are crucial for promoting sustainable energy solutions and improving the economic viability of solar energy systems [32].

The objective of this work is to enhance the available energy from the sun by utilizing a two-axis tracking device, which continuously makes the PV module align with the sun's rays. There are two methods for increasing the amount of solar radiation energy accessible. The first strategy is to absorb as much solar radiation as possible using the appropriate solar radiation-absorbing materials. The second method, presented in this work, is to use the optimization methodology for the solar photovoltaic panel over a day to increase radiations that reach the PV module. The optimization technique aims to maximize the PV panel's electrical power by tracking the sun's optimal tilt and azimuth angles. In this work, solar tracker optimization techniques like the Teaching learning-based optimization (TLBO) algorithm, Jaya algorithm, Rao-3 algorithm, Differential algorithm (DE), and Genetic algorithm (GA) are used. This work considers tilt and azimuth angles for a dual-axis solar tracker of a PV system, and the considered optimization algorithms

optimize it. The second aim of this work is to evaluate the optimum tilt-azimuth angle of the PV module using different algorithms. The purpose was to maximize the electrical power through the solar PV panel by tracking the sun's trajectories like azimuth and tilt angles throughout the day.

MATERIALS AND METHODS

A dual-axis solar tracker, as presented in Figure 1, is a mechanism designed to track the sun's trajectory in the sky, enabling it to make simultaneous adjustments in both horizontal (azimuth) and vertical (elevation) directions. This functionality allows the solar panel to maintain an optimal angle relative to the sun's position, thereby optimising its exposure and energy generation during the course of the day. This phenomenon leads to an enhancement in the efficacy of energy harvesting from photovoltaic panels.

TRAJECTORIES DETERMINED BY THE VARIOUS ALGORITHMS

Teaching Learning-Based Optimization (TLBO) Algorithm

Rao and Patel (2012) proposed the "Teaching Learning-Based Optimization" algorithm based on learning and teaching processes. The population size, number of generations, size, and other common regulating factors are required for the TLBO algorithm, whereas other algorithms require algorithm-specific control parameters.

There are two fundamental modes of algorithms: learners learning through teachers and learners interacting with

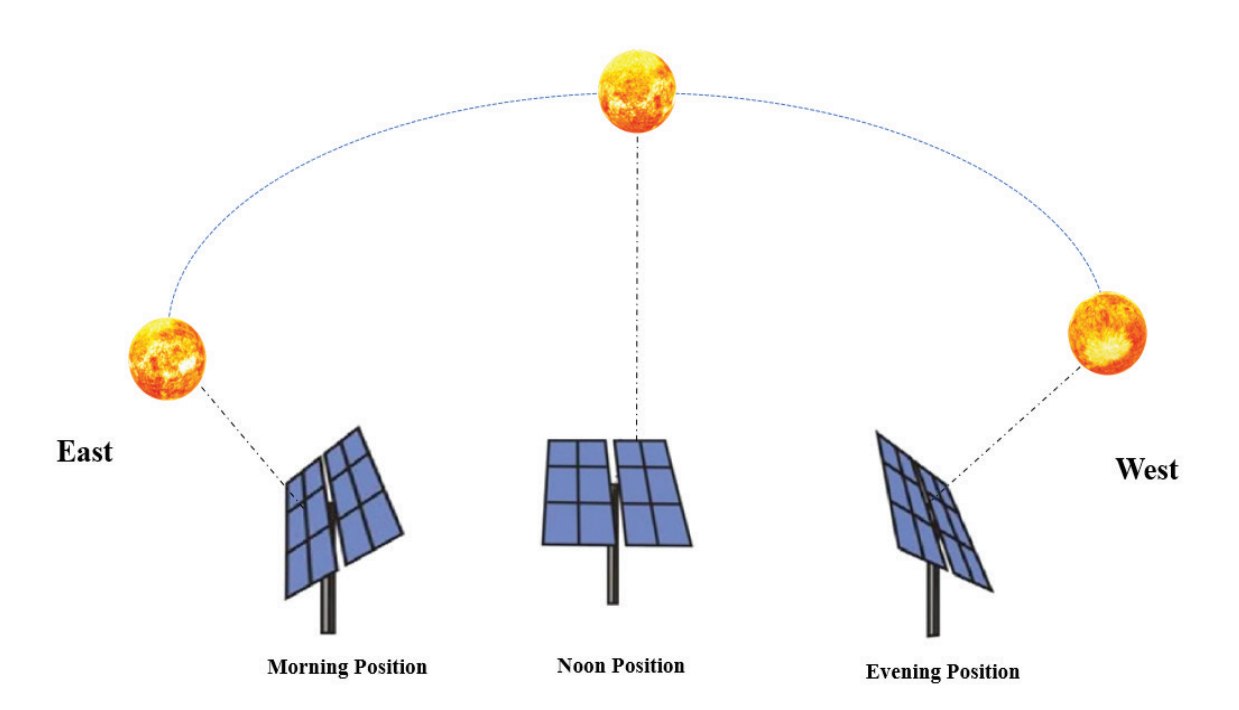


Figure 1. Schematic of dual-axis solar tracker.

other learners. The TLBO method considers a group of learners to be a population size, and different subjects presented to the group of learners to be different design factors for the given optimization problem, with the learners' outputs being the fittest value of the optimization problem. A teacher is regarded as the ideal solution among the general population. The design variable is a parameter included in the objective function of the given problem, and the best solution provides the best value for the objective function.

The working principle of the TLBO algorithm is given in Figure 2, [33].

JAYA Algorithm and Rao-3 Algorithm

The JAYA method is a new and easy optimization tool that addresses restricted and unconstrained difficulties, and its flowchart is represented in Figure 3 [34]. It is based on the best solution moving forward and the worst solution avoiding the population size N. The initial population for each design variable is created randomly within the lower

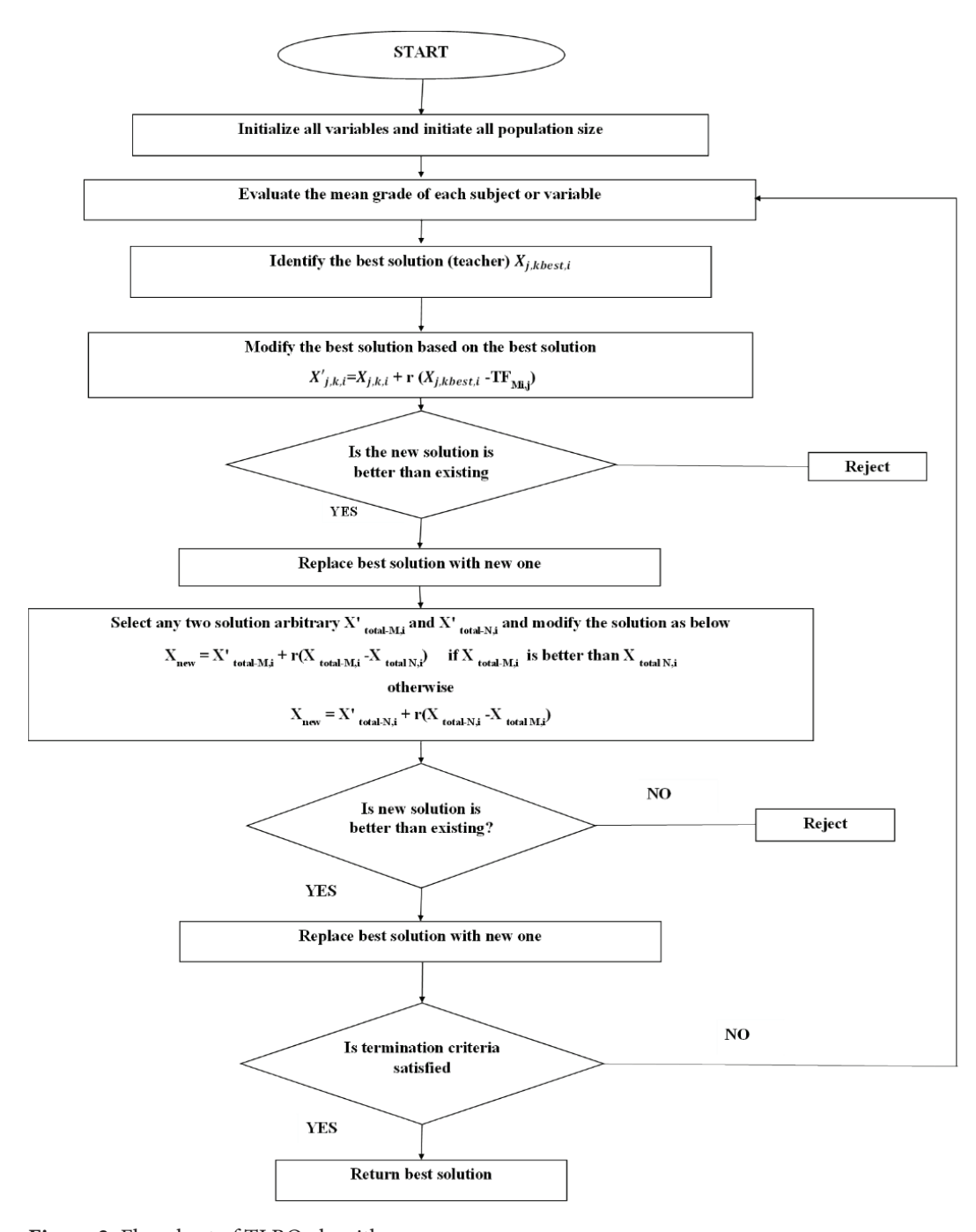


Figure 2. Flowchart of TLBO algorithm.

and upper bounds. Then, based on the idea of the best and worst candidate solutions within the population size, N, the values of the randomly generated variables are modified in each iteration. The main equation used in Jaya optimization algorithm is as follows by equation (1):

$$X'_{j,k,i} = X_{j,k,i} + r_{1,j,i} (X_{j,best,i} - |X_{j,k,i}|) - r_{2,j,i} (X_{j,worst,i} - |X_{j,k,i}|)$$
(1)

Where r_1 and r_2 are random numbers in the range [0,1], the function values at the end of each iteration become the next iteration's input value.

Rao and Pawar (2020) proposed the Rao-3 algorithm 2020 based on Quasi-oppositional. For the Rao-3 Algorithm, the modified equations used in optimization are as follows by equation (2) and its flowchart as shown in Figure 3, [35]:

$$X'_{j,k,i} = X_{j,k,i} + r_{1,j,i} (X_{j,best,i} - |X_{j,worst,i}|) + r_{2,j,i} (|X_{j,k,i} or X_{rand_{j,k,i}}| - (X_{rand_{j,k,i}} or X_{j,k,i}))$$
(2)

Differential Evolutionary (DE)

The differential evolution (DE) algorithm is a straightforward, effective, and efficient method for tackling global optimization problems. The effectiveness of the differential evolution algorithm is highly dependent on its mutation strategy, which is discussed in [10,36]. The flowchart of the DE algorithm is shown in Figure 4.

In the initialization, the initial population includes the 'N' solutions (i.e., size of the population member or size), and each population size contains a 'D' variable, where D is the design variable of search space. Therefore, the solution of the population member at generation 'G' is given as equation (3):

$$\begin{split} X_i^G &= \left(X_{i,1}, X_{i,2}, \ldots \ldots \ldots, X_{i,D}\right), \\ where, i &= 1, 2, 3, \ldots \ldots N \end{split} \tag{3}$$

The member's initial population should be spread across the entire search space. The initialization approach for member's solution that is most usually used as equation (4):

$$X_{i,j} = X_j^{min} + rand(0,1) * \left(X_J^{max} - X_j^{min}\right)$$
 (4)

Where X_{jmin} and X_{jmax} are the lower and upper bounds of the j_{th} dimension of the variable size, respectively, and rand (0,1) is a fundamental value between "0" and "1".

DE mutation strategy

DE/rand/1

The DE strategy used in the mutation, which is given by the equation (5):

$$V_i^G = X_{r,1}^G + F(X_{r,2}^G - X_{r,3}^G)$$
 (5)

Where r_1 , r_2 , and r_3 represent the distinct integer randomly generated within the range of [1, N], and F is the scaling factor used to determine the mutation scale. The scaling factor's range is restricted to (0,1).

Crossover operator

After mutation, the trial vector $U_i^G = (U_{i,1}^G, U_{i,2}^G, \dots, U_{i,D}^G)$ is created for each population, which is obtained by the equation (6):

$$U_{i,j}^{G} = \begin{cases} V_{i,j}^{G} & if \ randi, j(0,1) \le CR \ or \ j == jrand \\ X_{i,j}^{G} & otherwise \end{cases}$$
 (6)

Selection operator

Based on their fitness value, the selection operator selects whether the target vector survives and moves on to the next generation. The decision vector for the maximizing issue is as follows by the equation (7):

$$X_{i}^{G+1} = \begin{cases} U_{i}^{G} & \text{if } \left(fit \left(U_{i}^{G} \right) \leq fit(X_{i}^{G}) \right) \\ X_{i}^{G} & \text{otherwise} \end{cases}$$
 (7)

Genetic Algorithm (GA)

Holland, 1984, developed an algorithm known as a genetic algorithm that is based on Charles Darwin's theory of natural evolution. The natural selection of members of population size is the first step in the Genetic Algorithm (GA), a process of evolution. They give birth to children who carry their parents' genes, and these children's virtues

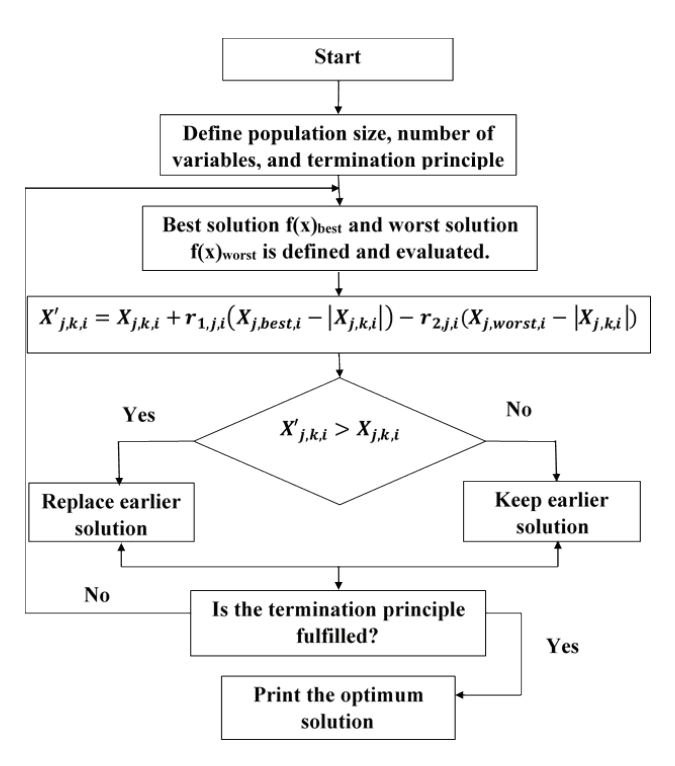


Figure 3. Flowchart of JAYA and Rao-3 algorithm.

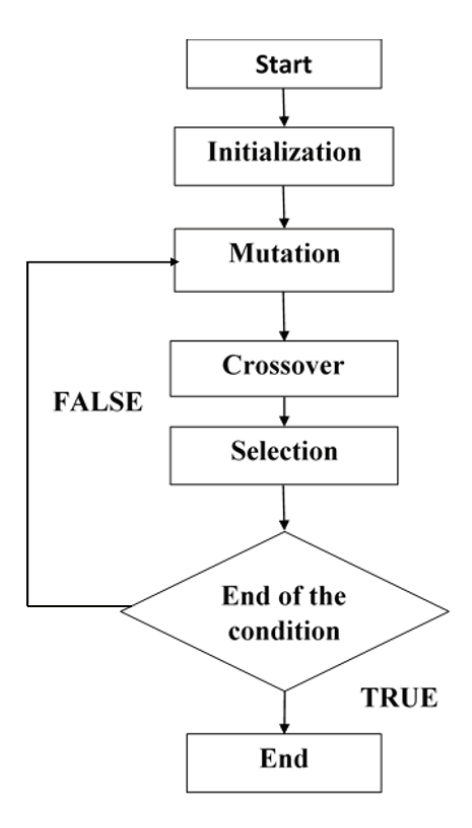


Figure 4. DE algorithm flow chart.

will be transmitted to the following generation. If the parents' qualities have a higher fitness value, their kids will outperform the parents' genes and have a better chance of survival. This algorithm will continue to iterate until the fittest individuals are identified. A genetic algorithm has five well-thought-out phases, as shown in Figure 5 [37].

The above-proposed algorithms are used to determine the total solar radiation at optimal tilt and azimuth angles. All of these methods used the same set of optimization parameters to find the best optimal solution. Our methods were designed to function together with a population size of 172 individuals, an iteration count of 1000, and two optimization variables, tilt angle and azimuth angle. In case of the Genetic algorithm, to encourage genetic variety in the population, we kept the crossover probability at 0.8 and the mutation scale factor at 0.5, facilitating the exploration of novel solution spaces.

Mathematical Model

By the mathematical model of the solar orbit and position and "Radiation maximization" demand, the objective function is:

$$Max(I_c(\beta,\gamma))$$
 (8)

Equation (1) represents the maximization of solar radiation (I_c) at an optimized azimuth angle (γ) and tilt angle (β).

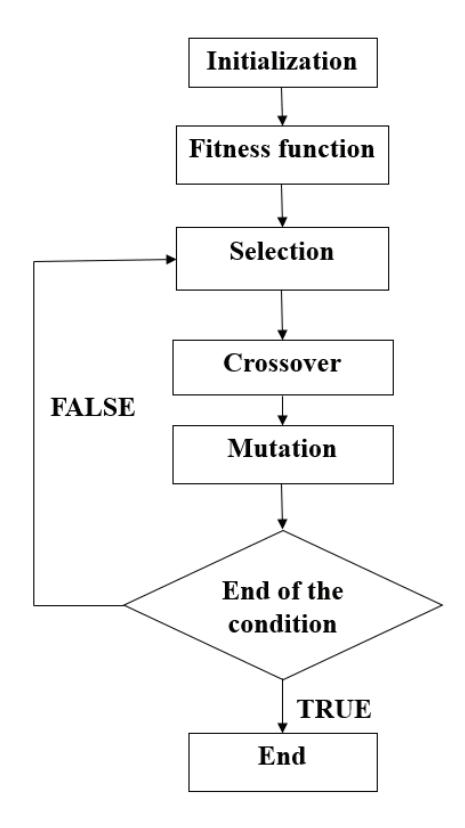


Figure 5. Flowchart of GA algorithm.

Constraints:

(i) Azimuth angle:

$$\gamma_{min} \le \gamma \le \gamma_{max} \tag{9}$$

Where γ_{min} & γ_{max} represents limits between the lower and upper limit values. In the optimization problem, the azimuth angle lies between [-110, 110].

(ii) Tilt angle:

$$\beta_{min} \le \beta \le \beta_{max} \tag{10}$$

Where β_{min} & β_{max} represent limits between the lower and upper limit values. The tilt angle optimization problem lies between [0°, 90°].

The calculation of electrical power generated within the PV system can be determined by integrating the instantaneous value of solar radiation received by the surface of the PV panel with specified time intervals. The system efficiency is influenced by different factors like tracking algorithms, solar radiation receiving effective surface area of the PV panel, changing time with the sun's movement throughout the day, and the DC/DC converter and inverter efficiency.

The solar radiation time-dependent for reaching the earth's surface depends on the extra-terrestrial sunlight-based radiation estimation, which is reduced by the quality of air present in the atmosphere. Lowering the values of the sun's radiation reaching the earth's surface are depicted as components of the sunbeam length through the atmosphere as clearness indices. On clear days, deliberate radiation from the sun on the surface of the earth and predicted extra-terrestrial solar beam develop their qualities over time.

The total radiation or instantaneous radiation (I_h) is the sum of the direct or beam radiation (I_{bh}) and the diffuse radiation on the horizontal surface (I_{dh}) as expressed in equation (11) [38].

$$I_h = I_{bh} + I_{dh} \tag{11}$$

The direct radiation on the horizontal surface (I_{bh}) and diffuse radiation on the horizontal surface (I_{dh}) depends on the Geographical location, day of the year, time, and weather situations. The lowering of solar radiation is increasing in tandem with the lengthening of the sun's ray pathways inside the atmosphere. The impact of the atmosphere on the scattering and absorption of radiation fluctuates over time due to changes in atmospheric conditions and air mass. Defining a standard "clear" sky and calculating the amount of radiation received on a horizontal surface during each hour and day under these standard conditions is beneficial. The estimation of solar beam radiation passes through clear atmosphere on a horizontal surface by considering the zenith angle (θ_z) and altitude for standard atmospheric circumstances. Therefore, the reduction of solar radiation is defined by the transmittance coefficient for beam (I_{bh}) and diffuse radiation (I_{dh}) for clear days, which are denoted by τ_b and τ_d , respectively, and can be calculated by the following equation [13,38]:

$$\tau_b = \frac{I_{bh}}{I_t} \tag{12}$$

And the estimation of the clear-sky diffuse radiation (I_{dh}) on horizontal surfaces are as follows:

$$\tau_d = \frac{l_d}{l_t} \tag{13}$$

Where transmittance coefficient for beam radiation can be calculated by the equation (14):

$$\tau_b = a_0 + a_1 \exp\left(\frac{-k}{\cos \theta_a}\right) \tag{14}$$

The values of the constants a_0 , a_1 , and k for the standard atmosphere with a visibility of 23 km are determined based on the values of a_0^* , a_1^* , and k^* , which are provided at altitudes below 2.5 km.

$$a_0^* = 0.4237 - 0.00821(6 - A)^2 \tag{15}$$

$$a_1^* = 0.5055 + 0.00595(6.5 - A)^2$$
 (16)

$$k^* = 0.2711 + 0.01858(2.5 - A)^2 \tag{17}$$

Where A is the altitude from the sea level in km, the constants a_0 , a_1 , and k can be calculated by applying the correction factors: $r_0 = \frac{a_0}{a_0^2}$, $r_1 = \frac{a_1}{a_1^2}$, and $r_k = \frac{k}{k^*}$. The values of correction factor are shown in table 1 for four different climatic types. Similarly, the transmittance coefficient for diffuse radiation on a horizontal surface during clear days can be calculated using the following equation (18):

$$\tau_d = 0.271 - 0.294\tau_b \tag{18}$$

Table 1. Correction factor for four different climates [Duffie et al. [38], with permission from John Wiley and sons].

Туре	r_0	r_1	r_k
Tropical	0.95	0.98	1.02
Mid-latitude summer	0.97	0.99	1.02
Sub-arctic summer	0.99	0.99	1.01
Mid-latitude winter	1.03	1.01	1.00

The average extra-terrestrial solar radiation is denoted by I_t , which is obtained by equation (19), [17,38]:

$$I_{t} = \frac{1}{\Delta t} \int_{t}^{t+\Delta t} I_{0}e(t) sin\alpha(t) dt$$
 (19)

Where, I_0 is the solar constant which is equal to 1367 w/m², and the eccentricity factor is given as equation (20), [38]:

$$e(t) = 1 + 0.034 \cos \frac{2\pi n}{365} \tag{20}$$

Where n represents the nth day of the year, counted from the first January. The total solar radiation represented by I_c in equation (14) is the function of the solar radiation (I_h), diffuse radiation (I_{dh}), and beam radiation (I_{bh}) on the surface of the PV panel with optimal tilt and azimuth angles for a different time is obtained as equation (21), [17,38]:

$$I_{c} = I_{bh} \frac{\cos i}{\sin \alpha} + I_{dh} \frac{(1 + \cos \beta)}{2} + \rho I_{h} \frac{(1 - \cos \beta)}{2}$$
 (21)

Where 'p' represents the ground reflectance factor and the value is 0.7, taken from Seme & Štumberger, 2011 and Seme et al., 2017, and 'i' represents the incidence angle of beam radiation from the sun to the solar PV surface. The relation between solar incidence angle and the other sun angles is obtained as equation (22), [38]:

$$\cos i = \cos \alpha \cos(\gamma_s - \gamma_w) \sin \beta + \sin \alpha \cos \beta \qquad (22)$$

Where ' γ_s , γ_w ' represents solar azimuth and wall azimuth angle, respectively, and ' α ' represents the altitude angle of

the sun, which is obtained as equation (23) and zenith angle is inverse of Sin α [38]:

$$\sin \alpha = \sin L \sin \delta_S + \cos L \cos \delta_S \cos \omega_S \tag{23}$$

And,

$$\omega_{\rm s} = 15^{\circ}(12 - T) \tag{24}$$

Where in above equations (23) & (24), L, δ_s , ω_s , & T represent the latitude angle for a particular geographical location, solar declination angle, solar hour angle, and solar time, respectively.

The integration of the electric energy for a given time interval $[t_1, t_2]$ gives the produced electrical energy by the following equation is given as equation (25), [38]:

$$E_{pv} = \eta_{pv} A_{pv} \int_{t_1}^{t_2} I_C(t) dt$$
 (25)

Where, in equation (25), E_{pv} , η_{pv} , A_{pv} , & I_C represent the PV system that has produced electrical energy. The total efficiency consists of the PV panel, dc/dc converter and inverter, active surface area of the panel, and total solar radiation during a predefined time interval $[t_1, t_2]$, respectively.

RESULTS AND DISCUSSION

This section deals with the results obtained during the optimization of dual axis solar tracker for a PV module in order to achieve maximum solar radiation at optimum tilt-azimuth angles and further maximize the electrical energy by using optimization algorithms like JAYA algorithm, Teaching learning-based optimization (TLBO) algorithm, Rao-3 algorithm, Differential evolutionary algorithm (DE) and Genetic algorithm (GA). The codes of algorithms were run in MATLAB software to determine the

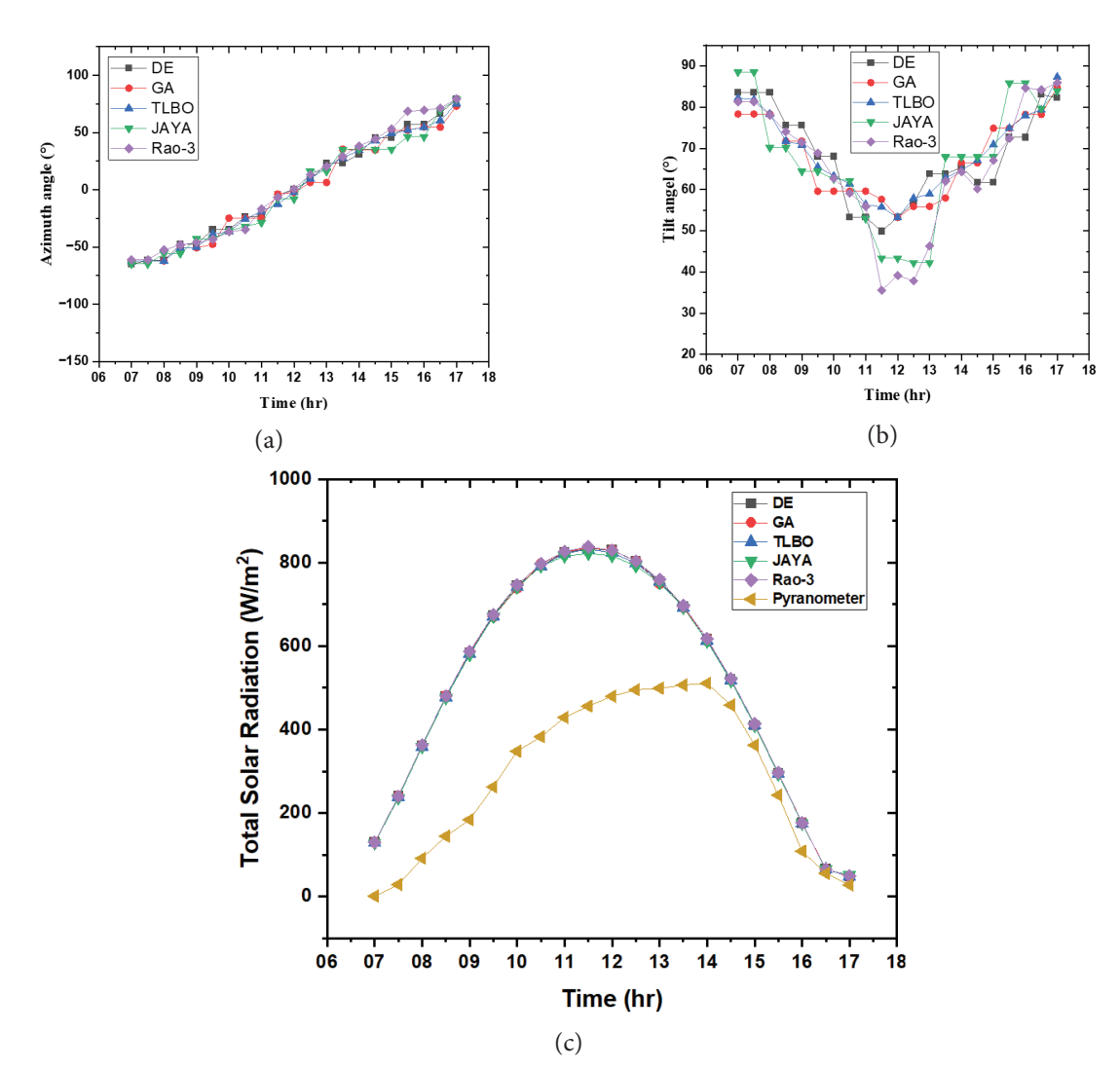


Figure 6. Results for winter day, n^{th} =350, at Surat city: (a) Optimum Azimuth angle β v/s time, (b) Optimum tilt angle β v/s time, and (c) Total solar radiation determined by proposed algorithms and Pyranometer.

optimum azimuth and tilt angles to obtain the maximum solar radiation tracked.

The trajectory of the solar tracker depends upon the mathematical modeling, geographical location (i.e., Latitude and longitude), solar time, and date for the particular location. In this work, the data were taken for the location of Surat city, India, which comes under tropical climate type: Latitude=21.1702° N, Longitude=72.8311° E. The lower and upper limits of solar tilt angles are $[0^0, 90^0]$, and for solar azimuth angles are [-110°, 110°] over a day from 7 AM to 5 PM. By implementing the parameters mentioned above into the optimization algorithms for Winter Days, nth = 350, Summer Days, nth = 136, and spring Days, nth = 58 to determine the total solar radiation at optimum tilt angle and solar azimuth angle for a dual-axis solar tracker. The optimization results show the total solar radiation variation for optimum tilt and azimuth angles throughout the day. The total solar radiation exhibits a progressive increase until reaching its peak at noon, followed by a fall from 7

AM to 5 PM when the optimal tilt and azimuth angles are employed. The study examines the variability of total solar radiation and determines the optimal tilt-azimuth angles for different algorithms.

Figure 6 (a) represents the result of the optimum azimuth angle on winter days ($n^{th}=350$ days of the year), which vary between -110° to 110° with the different times from sunrise to sunset. The azimuth angle is negative azimuth angle before noon, zero at noon, and positive azimuth angle in the afternoon. Figure 6 (b) represents the result of the optimum tilt angle, which is determined by the above-proposed algorithm for the winter days ($n^{th}=350$ days of the year). The tilt angle varies between [0^0 , 90^0], and the tilt angle minimum at the noon position. Figure 6 (c) shows the result of optimum solar radiation for the winter days (i.e., $n^{th}=350$ days of the year) by the above optimization algorithms. The maximum solar radiation for the dual-axis tracking system was obtained at different optimum tilt angles and azimuth angles. In addition, the amount of

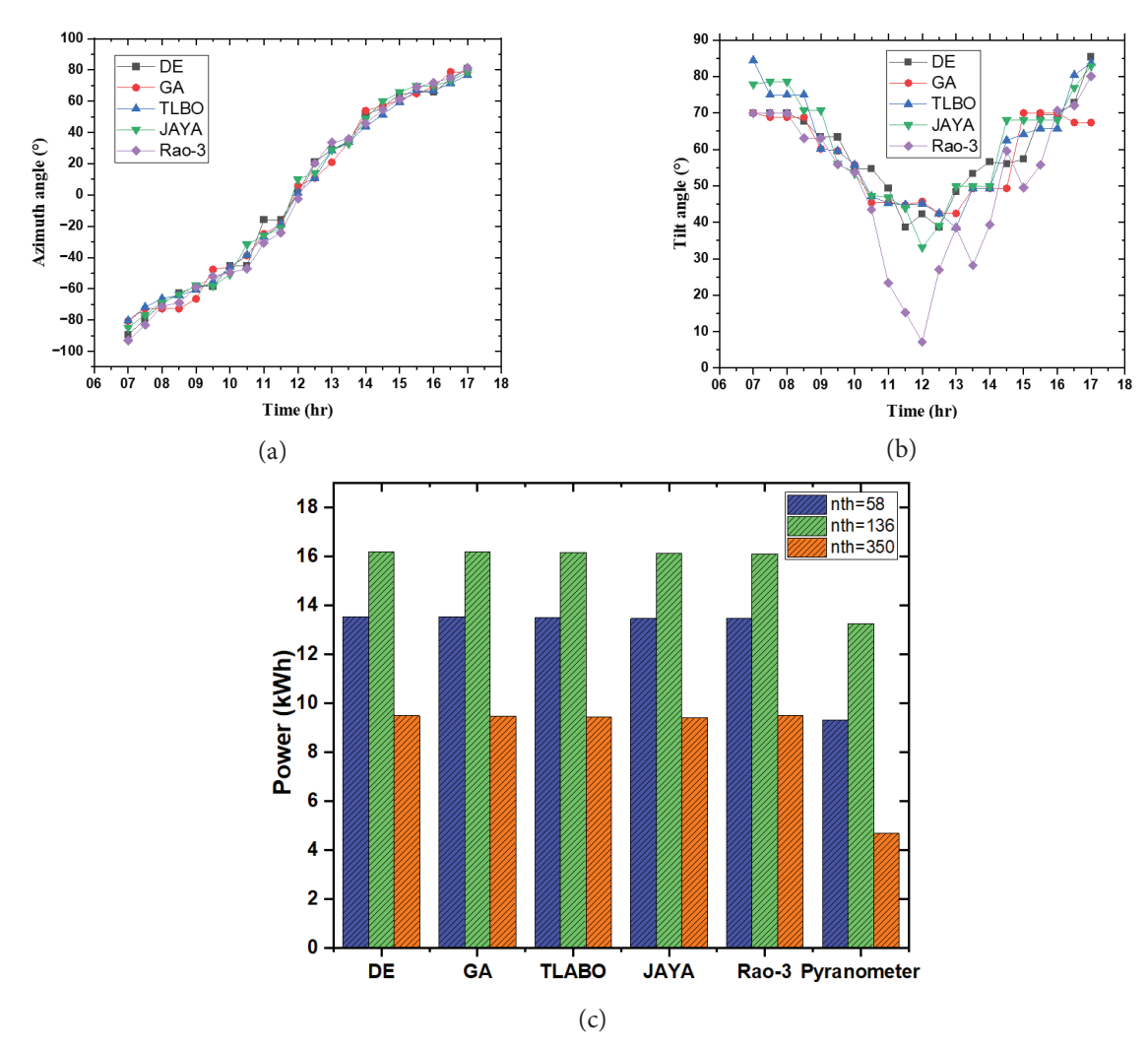


Figure 7. Comparative results of electrical power for spring day (58th), summer days (136th), and winter day (350th) of Surat city (coordinates: 21.1702° N, 72.8311° E), determined by various algorithms and measured.

electrical energy that is contained within the PV panel was evaluated and depicted in Figure 7. This was determined using calculations based on a polycrystalline PV panel with an active area of 15.32 m^2 and a total efficiency of 12 %.

Figure 8 (a) represents the optimized value of azimuth angle throughout the day on a typical summer day in Surat City. It can be seen that the results obtained for DE, GA, TLBO, JAYA, and Rao-3 algorithms are almost same. The variation in tilt angles are given in Figure 8 (b), the curves are forming a valley shaped structure with the peakpeak value given by different algrithm. Figure 8 (c), as shown above, represents the maximum tracked total solar radiation for the dual axis tracker obtained at optimum azimuth and tilt angle, as shown in Figure 7 (a) and Figure 7 (b), respectively, determined by the use of optimization algorithms from 7 AM to 5 PM. At the optimized angles, the variation of solar radiation throughout the day is shown in Figure 7 (c). Further, the electrical energy in the PV panel was evaluated, as shown in Figure 9. This was calculated for a polycrystalline PV panel with an active area and total efficiency of 15.32 m² and 12%, respectively.

Figure 9 (c) represents the result for the maximum solar radiation obtained at optimum tilt and azimuth angle as shown in Figure 9 (a) and (b), respectively, at Surat city coordinates 21.1702° N, 72.8311° E for the 136° day of the year. The results of total solar radiation obtained by the proposed method compared with the result obtained by measured data by pyranometer, which is more than the measured data. Further calculations for the PV panel's electrical output, as depicted in Figure 7, were made using a polycrystalline PV panel with an active surface area of 15.32 m² and a total efficiency of $\eta = 0.12$ (including the PV panel, dc/dc converters, and inverter).

The electrical energy calculation was based on total solar radiation for a 2.5 kW photovoltaic (polycrystalline silicon PV) system with an active surface area of 15.32 m². The total measured efficiency, which contains the efficiency for solar photovoltaic (PV) panels, dc/dc converters, and MPPT inverters, is $\eta = 0.12$ [17]. The results show that the dual-axis solar tracker gives additional output power than the measured.

The Electrical power for the tracked system at Surat city, India, for spring days, summer days, and winter days for different algorithms are as under: For spring days, the electrical power generation by different optimization algorithms are as follows: TLBO-13.4953 kWh, JAYA-13.4664 kWh, Rao-3-13.4805 kWh, DE-13.5539 kWh, and GA-13.5437 kWh. These results demonstrate notable enhancements compared to the electrical output of the measured fixed system, which stands at 9.3150 kWh. For summer days, the electrical power generation by different optimization algorithms are as follows: TLBO-16.1713 kWh, JAYA-16.1436 kWh, Rao-3-16.1125 kWh, DE-16.2079 kWh, and GA-16.1969 kWh. These results demonstrate notable enhancements compared to the electrical output of the measured fixed system, which stands at 13.2610 kWh. For winter days, the electrical power generation by different optimization algorithms are as follows: TLBO-9.4490 kWh, JAYA-9.4071 kWh, Rao-3-9.5174 kWh, DE-9.4881 kWh, and GA-9.4846 kWh. These results demonstrate notable enhancements compared to the electrical output of the measured fixed system, which stands at 4.3852 kWh.

The optimization algorithms are compared with that of Seme et al. 2011 [9, 10]. The results are obtained for Slovenia, Maribor $(46^{\circ}33'N, \text{ and } 15^{\circ}39'E)$, as shown in Figure 10, and was found to be in good agreement. It is now

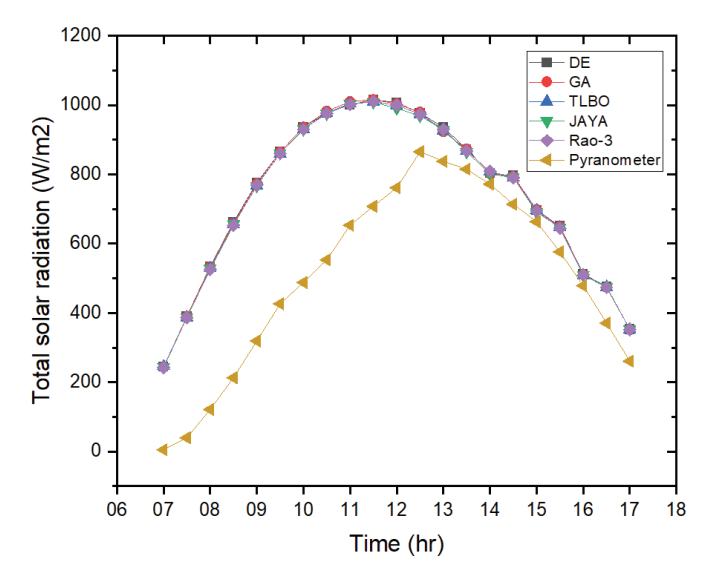


Figure 8. Results for spring Day, n^{th} =58, at Surat city: (a) Optimum Azimuth angle β v/s time, (a) Optimum tilt angle β v/s time, and (c) Total solar radiation determined by proposed algorithms and Pyranometer.

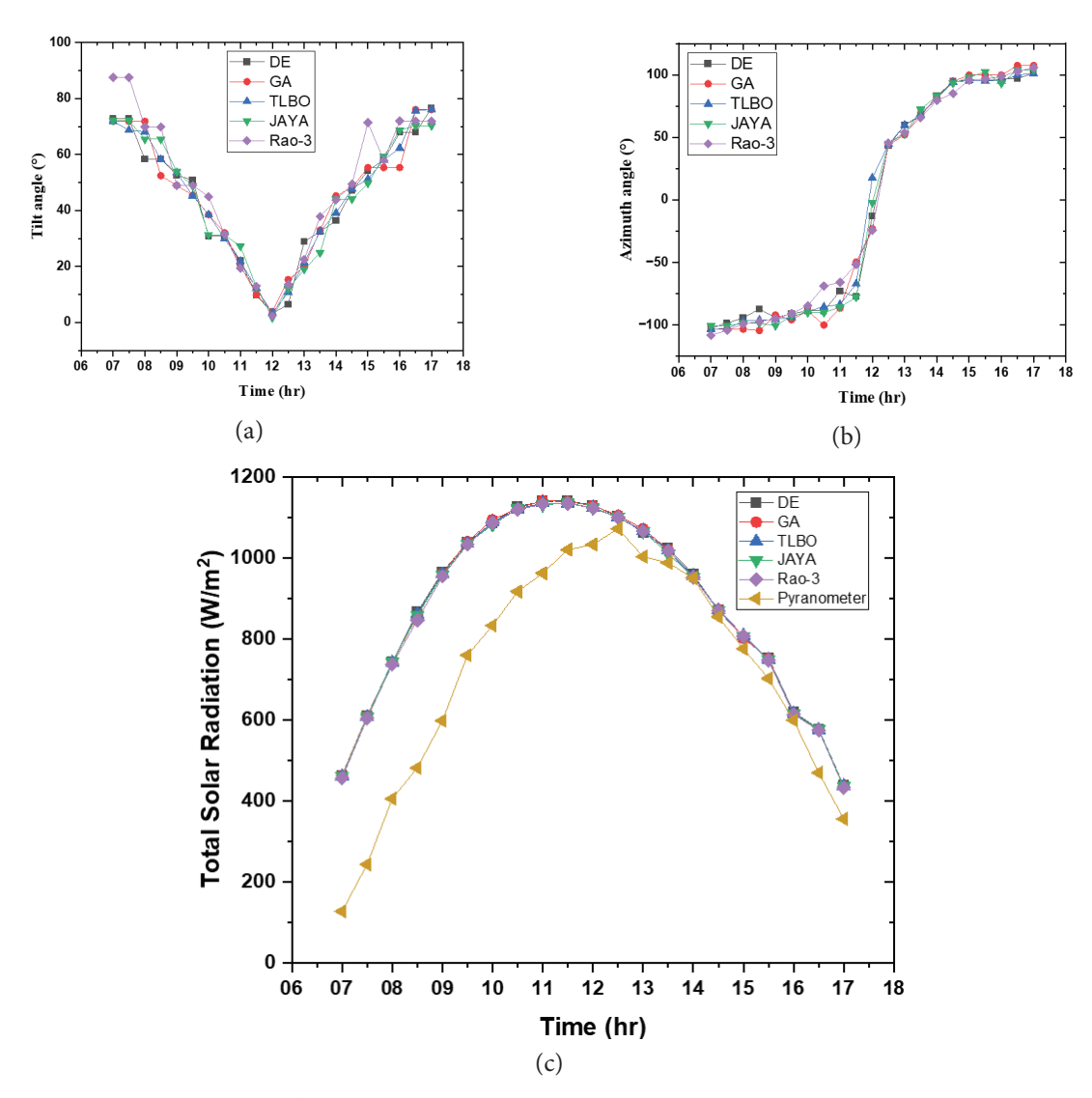


Figure 9. Results for summer day, n^{th} =136, at Surat city: (a) Optimum tilt angle β v/s time, (b) Optimum Azimuth angle β v/s time, (c) Total solar radiation determined by proposed algorithms and Pyranometer.

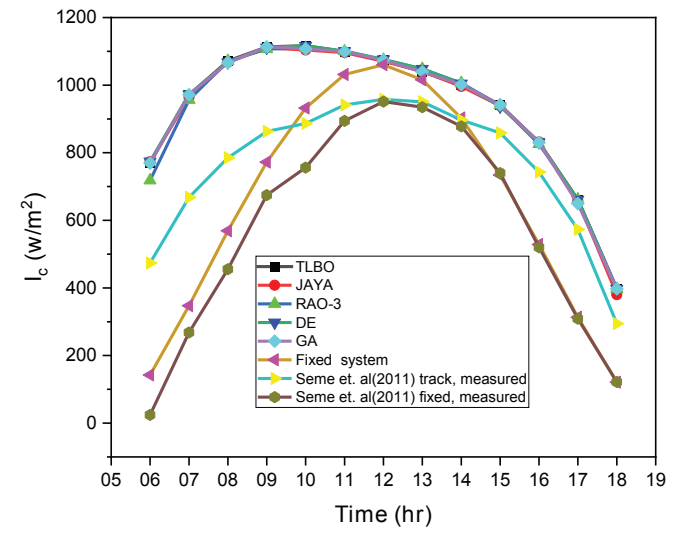


Figure 10. comparative results for summer days, nth=199: The solar radiation for the city Maribor, Slovenia (coordinates: 46° 33' N & 15° 39' E), track measured and fixed measured with the calculated tracked and fixed system (at a constant angle, β =24°) determined by various algorithms.

shown that the dual-axis solar tracker gives additional output power than the fixed system.

CONCLUSION

The present study was to optimise solar radiation absorption by photovoltaic (PV) modules in order to increase the amount of energy derived from sunlight reaching their surface. A non-linear and bounded optimisation problem is utilised to assess the optimal paths of tilt angle and sun azimuth angle. Following are the conclusions that may be drawn from this work:

- The objective function is in the form of an explicit function that is not known. Optimization method like the TLBO algorithm, JAYA algorithm, Rao-3 algorithm, DE algorithm, and GA algorithm have been utilised for the purpose of assessing the objective function. The electrical power increment achieved by various proposed algorithms, such as TLBO Algorithm, JAYA Algorithm, Rao-3 Algorithm, Differential Evolution Algorithm, and Genetic Algorithm, in comparison to a measured fixed system, demonstrated significant enhancements in power generation.
- The optimization results for different algorithms show that the output electrical power with the dual-axis tracker is more than that of the fixed system.
- The Electrical power for the tracked system at Surat city, India, for spring days, summer days, and winter days for different algorithms are as follows. For spring days, the electrical power generation by different optimization algorithms are TLBO-13.4953 kWh, JAYA-13.4664 kWh, Rao-3-13.4805 kWh, DE-13.5539 kWh, GA-13.5437 kWh, and measured fixed system-9.3150 kWh
- For summer days, the electrical power generation by different optimization algorithms are as follows: TLBO-16.1713 kWh, JAYA-16.1436 kWh, Rao-3-16.1125 kWh, DE-16.2079 kWh, and GA-16.1969 kWh, and measured fixed system-13.2610 kWh.
- For winter days, the electrical power generation by different optimization algorithms are as follows: TLBO-9.4490 kWh, JAYA-9.4071 kWh, Rao-3-9.5174 kWh, DE-9.4881 kWh, and GA-9.4846 kWh, and measured fixed system-4.3852 kWh.
- The results obtained through the algorithms were compared with the experimental results from the literature for Maribor, Slovenia, and found to be in good agreement.
- The optimization algorithm based dual axis tracker greatly improves the solar energy trapped for industrial applications like drying, hot water generation, building heating, and power generation.
- The integration of Internet of Things (IoT) with a dualaxis solar tracker further helps in large solar farms so that they can be remotely monitored, diagnosed, and operated.

NOMENCLATURE

 β Tilt angle

γ Azimuth angle

α Altitude angle

ρ Ground reflectance factor

i Incidence angle

 δ_s Solar declination angle

 ω_s Solar hour angle

 $[t_1, t_2]$ Time interval

N Population size

I Solar radiation

l Sunbeam path length

K Clearness indices

 I_0 Solar constant (1367 w/m²)

L Latitude angle

T Solar time

E_{nv} Electrical energy by PV system

 η_{pv} Efficiency of PV panel

 \hat{A}_{py} Surface area of PV panel

Subscript

Max Maximum

Meas Measured

Min Minimum

n nth day of the year

Abbreviation

TLBO Teaching Learning Based Optimization

GA Genetic Algorithm

DE Differential Evolution

PV Photovoltaic

ACKNOWLEDGMENT

This research is funded by the Sardar Vallabhbhai National Institute of Technology Surat (SVNIT Surat) through SEED Money Project No. 2020-21/ Seed Money/34. The authors are grateful to the Director, SVNIT Surat, for his constant support.

AUTHORSHIP CONTRIBUTIONS

Authors equally contributed to this work.

DATA AVAILABILITY STATEMENT

The authors confirm that the data that supports the findings of this study are available within the article. Raw data that support the finding of this study are available from the corresponding author, upon reasonable request.

CONFLICT OF INTEREST

The author declared no potential conflicts of interest with respect to the research, authorship, and/or publication of this article.

ETHICS

There are no ethical issues with the publication of this manuscript.

STATEMENT ON THE USE OF ARTIFICIAL INTELLIGENCE

Artificial intelligence was not used in the preparation of the article.

REFERENCE

- [1] Green MA. Photovoltaics: technology overview. Energy Policy 2000;28:989–998. [CrossRef]
- [2] Dubey S, Sarvaiya JN, Seshadri B. Temperature dependent photovoltaic (PV) efficiency and its effect on PV production in the world: a review. Energy Procedia 2013;33:311–321. [CrossRef]
- [3] Wysocki JJ, Rappaport P. Effect of temperature on photovoltaic solar energy conversion. J Appl Phys 1960;31:571–578. [CrossRef]
- [4] Koundinya S, Vigneshkumar N, Krishnan AS. Experimental study and comparison with the computational study on cooling of PV solar panel using finned heat pipe technology. Mater Today Proc 2017;4:2693–2700. [CrossRef]
- [5] Al-Rousan N, Isa NAM, Desa MKM. Advances in solar photovoltaic tracking systems: a review. Renew Sustain Energy Rev 2018;82:2548–2569. [CrossRef]
- [6] Rathore A. Energy, exergy and performance analysis of a 380 kWP roof-top PV plant assisted with data-driven models for energy generation. J Therm Eng 2024;10:1164–1183. [CrossRef]
- [7] Mousazadeh H, Keyhani A, Javadi A, Mobli H, Abrinia K, Sharifi A. A review of principle and sun-tracking methods for maximizing solar systems output. Renew Sustain Energy Rev 2009;13:1800–1818. [CrossRef]
- [8] Abdallah S, Badran OO. Sun tracking system for productivity enhancement of solar still. Desalination 2008;220:669–676. [CrossRef]
- [9] Seme S, Štumberger G. A novel prediction algorithm for solar angles using solar radiation and differential evolution for dual-axis sun tracking purposes. Sol Energy 2011;85:2757–2770. [CrossRef]
- [10] Seme S, Štumberger G, Voršič J. Maximum efficiency trajectories of a two-axis sun tracking system determined considering tracking system consumption. IEEE Trans Power Electron 2011;26:1280–1290.

 [CrossRef]
- [11] Alayi R, Harasii H, Pourderogar H. Modeling and optimization of photovoltaic cells with GA algorithm. J Robot Control 2020;2:35-41. [CrossRef]
- [12] Perini S, Tonnellier X, King P, Sansom C. Theoretical and experimental analysis of an innovative dual-axis tracking linear Fresnel lenses concentrated solar thermal collector. Sol Energy 2017;153:679–690. [CrossRef]

- [13] Zlatanov H, Weinrebe G. CSP and PV solar tracker optimization tool. Energy Procedia 2014;49:1603–1611. [CrossRef]
- [14] León N, García H, Ramírez C. Semi-passive solar tracking concentrator. Energy Procedia 2014;57:275–284. [CrossRef]
- [15] Ferdaus RA, Mohammed MA, Rahman S, Salehin S, Mannan MA. Energy efficient hybrid dual axis solar tracking system. J Renew Energy 2014;2014:1–12.
- [16] Sidek MHM, Azis N, Hasan WZWB, Ab Kadir MZA, Shafie S, Radzi MAM. Automated positioning dual-axis solar tracking system with precision elevation and azimuth angle control. Energy 2017;124:160–170. [CrossRef]
- [17] Seme S, Srpčič G, Kavšek D, Božičnik S, Letnik T, Praunseis Z, et al. Dual-axis photovoltaic tracking system: design and experimental investigation. Energy 2017;139:1267–1274. [CrossRef]
- [18] Awasthi A, Shukla AK, M S, Dondariya C, Shukla KN, Porwal D, et al. Review on sun tracking technology in solar PV system. Energy Rep 2020;6:392–405. [CrossRef]
- [19] Guo M, Zang H, Gao S, Chen T, Xiao J, Cheng L, et al. Optimal tilt angle and orientation of photovoltaic modules using HS algorithm in different climates of China. Appl Sci 2017;7:1028. [CrossRef]
- [20] Fahad HM, Islam A, Islam M, Hasan MF, Brishty WF, Rahman MM. Comparative analysis of dual and single axis solar tracking system considering cloud cover. In: 2019 International Conference on Energy and Power Engineering (ICEPE). IEEE; 2019. p. 1–5.
- [21] Zaher A, Traore A, Thiéry F, Talbert T, Shaer B. Optimization of solar tracking systems. Int J Energy Power Eng 2018;12:367-371.
- [22] Saymbetov A, Mekhilef S, Kuttybay N, Nurgaliyev M, Tukymbekov D, Meiirkhanov A, et al. Dualaxis schedule tracker with an adaptive algorithm for a strong scattering of sunbeam. Sol Energy 2021;224:285–297. [CrossRef]
- [23] Al-Amayreh MI, Alahmer A. On improving the efficiency of hybrid solar lighting and thermal system using dual-axis solar tracking system. Energy Rep 2022;8:841–847. [CrossRef]
- [24] Mamodiya U, Tiwari N. Dual-axis solar tracking system with different control strategies for improved energy efficiency. Comput Electr Eng 2023;111:108920. [CrossRef]
- [25] Muthukumar P, Manikandan S, Muniraj R, Jarin T, Sebi A. Energy efficient dual axis solar tracking system using IoT. Meas Sens 2023;28:100825. [CrossRef]
- Pirayawaraporn A, Sappaniran S, Nooraksa S, Prommai C, Chindakham N, Jamroen C. Innovative sensorless dual-axis solar tracking system using particle filter. Appl Energy 2023;338:120946. [CrossRef]

- [27] Anshory I, Jamaaluddin J, Fahruddin A, Fudholi A, Radiansah Y, Subagio DG, et al. Monitoring solar heat intensity of dual axis solar tracker control system: new approach. Case Stud Therm Eng 2024;53:103791. [CrossRef]
- [28] Flores-Hernández DA, Islas-Estrada LR, Palomino-Resendiz SI. A novel tracking strategy based on real-time monitoring to increase the lifetime of dual-axis solar tracking systems. Appl Sci 2024;14:8281.

 [CrossRef]
- [29] Koshkarbay N, Mekhilef S, Saymbetov A, Kuttybay N, Nurgaliyev M, Dosymbetova G, et al. Adaptive control systems for dual axis tracker using clear sky index and output power forecasting based on ML in overcast weather conditions. Energy AI 2024;18:100432. [CrossRef]
- [30] Praveen PN, Menaka D. A dual-axis solar tracking system with minimized tracking error through optimization technique. Multimed Tools Appl 2023;83:58891–58914. [CrossRef]
- [31] Bousbia Salah SE, Benseddik A, Meneceur N, Zine A, Deghoum K. Design and realization of a new solar dryer assisted by a parabolic trough concentrator (PTC) with a dual-axis solar tracker. Sol Energy 2024;283:113001. [CrossRef]

- [32] Kumba K, Upender P, Buduma P, Sarkar M, Simon SP, Gundu V. Solar tracking systems: advancements, challenges, and future directions: a review. Energy Rep 2024;12:3566–3583. [CrossRef]
- [33] Rao RV, Patel V. An elitist teaching-learning-based optimization algorithm for solving complex constrained optimization problems. Int J Ind Eng Comput 2012;3:535–560. [CrossRef]
- [34] Venkata Rao R. Jaya: a simple and new optimization algorithm for solving constrained and unconstrained optimization problems. Int J Ind Eng Comput 2016;7:19–34. [CrossRef]
- [35] Rao RV, Pawar RB. Quasi-oppositional-based Rao algorithms for multi-objective design optimization of selected heat sinks. J Comput Des Eng 2020;7:830–863. [CrossRef]
- [36] Differential evolution. Berlin/Heidelberg: Springer-Verlag; 2005.
- [37] Holland JH. Genetic algorithms and adaptation. In: Adaptive control of ill-defined systems. Boston: Springer US; 1984. p. 317–333. [CrossRef]
- [38] Duffie JA (deceased), Beckman WA, Blair N. Solar engineering of thermal processes, photovoltaics and wind. Wiley; 2020. [CrossRef]